

RESEARCH

Safe, efficient and socially-compatible decision of automated vehicles: a case study of unsignalized intersection driving

Daofei Li*, Ao Liu, Hao Pan and Wentao Chen

*Correspondence: dfli@zju.edu.cn
Institute of Power Machinery and
Vehicular Engineering, Faculty of
Engineering, Zhejiang University,
No. 38 Zheda Road, Xihu District,
310027, Hangzhou, China
Full list of author information is
available at the end of the article

Abstract

Safe and smooth interacting with other vehicles is one of the ultimate goals of driving automation. However, recent reports of demonstrative deployments of automated vehicles (AVs) indicate that AVs are still difficult to meet the expectation of other interacting drivers, which leads to several AV accidents involving human-driven vehicles (HVs). This is most likely due to the lack of understanding about the dynamic interaction process, especially about the human drivers. By investigating the causes of 4,300 video clips of traffic accidents, we find that the limited dynamic visual field of drivers is one leading factor in inter-vehicle interaction accidents, especially in those involving trucks. A game-theoretic decision algorithm considering social compatibility is proposed to handle the interaction with a human-driven truck at an unsignalized intersection. Starting from a probabilistic model for the visual field characteristics of truck drivers, social fitness and reciprocal altruism in the decision are incorporated in the game payoff design. Human-in-the-loop experiments are carried out, in which 24 subjects are invited to drive and interact with AVs deployed with the proposed algorithm and two comparison algorithms. Totally 207 cases of intersection interactions are obtained and analyzed, which shows that the proposed decision-making algorithm can not only improve both safety and time efficiency, but also make AV decisions more in line with the expectation of interacting human drivers. These findings can help inform the design of automated driving decision algorithms, to ensure that AVs can be safely and efficiently integrated into the human-dominated traffic.

Keywords: Automated driving; Social compatibility; Game theory; Interactive driving; Unsignalized intersection

1 Introduction

Automated driving (AD) is evolving rapidly in recent years. By assisting human drivers in driving tasks, e.g. lane keeping and speed control, AD has achieved much success in commercialization. Further, the last five years have witnessed the rapid development of autonomous driving technology, e.g. RoboTaxi, which has attracted much attention from both the public and the research community. Although AD is often advertised as a safety and comfort feature in modern vehicles, the current AD technologies have still raised many safety concerns related to human factors [1]. Without resolving safety concerns and achieving stable driving performances, AD is still far away from winning wide trust from users [2–5]. As pointed out by Noy et

al. [6], AD should be designed in accordance to cybernetics principles, i.e. by using a human-centric approach in technology development.

Such human-centric approach does not mean to consider only the human driver/passenger in AV, but also those traffic participants outside the AV cabin. In the foreseeable future, highly automated vehicles are hopefully to share the open roads with human-driven vehicles (HVs). Considering the infinite varieties of human driving behaviors, it is challenging for AVs to safely and efficiently interact with HVs in dynamic scenarios [7]. Concerns over the harmonious coexistence of AVs and HVs have been raised by both the academics and industries [8]. Public safety reports indicate that current AVs are driving in unexpected ways from human drivers' point of view, which leads to several traffic accidents. A road test report by Waymo also shows that the human driver is the critical factor in the interactions between AVs and HVs, posing a significant threat to AVs' safety [9]. However, available driving decision-making algorithms have not sufficiently considered the interactions between AVs and HVs [10]. Therefore, there is an urgent need for research on decision-making of automated vehicles in highly dynamic and interaction-intensive driving scenarios.

In current AV decision algorithms, there have been basically two ways to consider inter-vehicle interactions. A common way is to directly imitate the cooperation and interaction behaviors of human drivers. For example, Beaucorps et al. [11] obtained some reference speed profiles of specific styles based on human driving data clustering, which were used to achieve human-like driving in complex interactions. Chen et al. [12] proposed an imitation learning framework to design the driving policy for complex urban scenarios. Theoretically, given sufficient interaction data of human driving, such models can provide a satisfactory driving policy that considers social compatibility. However, the imitation-based methods are limited by the completeness of dataset, making them difficult to cope with the corner cases not covered.

Another way is to make interactive decisions and planning based on predicting the interacting vehicle's future behaviors [13–19]. For example, Sezer et al. [13] handled the interaction problem by predicting the interacting driver's intents with uncertainties, while the parameters of the driver behavior model were selected intuitively, and the human decision mechanism was not considered. Menendez-Romero et al. [14] proposed a cooperative driving strategy to consider AV's safety and comfort expectations, and also the conflict vehicle's efficiency in merging at highway ramps. An intention prediction algorithm is integrated to provide the system with a "courtesy" behavior. Wang [15] modeled the interaction at unsignalized intersections using utility functions of safety and efficiency. The algorithm predicts the other vehicle's driving directions and calculates the optimal speed planning by analyzing the possible collision points. However, the utility settings do not include the characteristics, such as intent and other psychological factors. To summarize, these prediction-based approaches can model how the AV should respond with social compatibility, if the interacting vehicle behaves as predicted. However, in dynamic scenarios with intense two-way interactions, the interacting vehicle may be influenced by the AV maneuvers and deviate from the predicted motion, which should be further addressed. As pointed out by a recent review on vehicle motion prediction [20], to accommodate highly dynamic interactions between ego vehicle and other

traffic participants, the coordination between motion prediction and ego-motion planning is one of the major challenges.

The existing literatures have clarified that a clear understanding of other traffic users is key to safe and efficient driving in interaction-intensive scenarios. However, there are only limited studies on socially compatible decision algorithms for AV. Among them, game theory has been often applied to the interactive decision-making involving multiple traffic participants [21–28]. These approaches formulate an AV decision problem in an integrated framework by considering all players simultaneously, with which the game payoff design can also be viewed as one special case of prediction-based methodology. For example, Li et al. [21] presented a Leader-Follower game-theoretic algorithm for various parametrized intersection scenarios. Wang et al. [26] proposed an integrated prediction and planning framework that allows the AVs to infer the characteristics of other road users. By learning the weights of selfish, altruistic and mediocre driving behaviors, the socially compatible reward is constructed, which optimizes not only AV's own rewards, but also its courtesy to others. In our previous work [27], Prospect Theory is incorporated for the payoff design in an unsignalized intersection game with two or four vehicles. In [28], we developed a level-k game model for the overtaking behaviours on two-lane two-way highways. In summary, game-theoretic decision algorithms has shown promising performances in modelling human-like decisions. However, there is an urgent need on how to develop a design method for decision payoff of drivers, especially in complex and interactive driving contexts.

Therefore, many crucial questions related to interactive driving need to be answered. For example, what are the key influencing factors of social compatibility that need to be considered in inter-vehicle interactions? How can social compatibility be realized in AV decision? When interacting with HVs, will social compatibility improve the decision performance of AV, e.g. safety and human driver's acceptance?

To address these challenges, in this research we attempt to incorporate such social compatibility in the AV decision algorithm, with a specific focus on the visual limitation of interacting human drivers. The contribution of this paper is two-fold.

- 1 A probabilistic model of the truck driver's visual field is constructed and applied in AV decision design. The model can estimate the probability of AV being observed by the HV driver during the interaction process. To the best of our knowledge, this is the first attempt to consider the visual limitation of interacting HV drivers in an AV decision algorithm.
- 2 A game-theoretic framework is proposed to incorporate social compatibility into AV decision, for which the safety and efficiency improvements over commonly-used algorithms are validated via human-in-the-loop experiments.

The rest of the paper is organized as follows. Section 2 briefs the research's motivation, constructs the AV visibility model and introduces the socially compatible decision algorithm. Section 3 details the driving simulator experiment design, while the results and discussions are summarized in Section 4. Finally, Section 5 concludes the paper and discusses some potential future work.

2 Method

2.1 Motivation

As defined by Ladegård [29], social compatibility (SC) is the integration of social fitness and reciprocity, which represents an agent's responsiveness in social interactions. Similar to daily interpersonal interactions, interactive driving in traffic, as a kind of interaction on wheels, also needs SC in decision-making. The realization of SC in driving decision should be based on perception and prediction of other road users. In other words, an inter-vehicle interaction starts from the perception of each other. Among other things, visual perception plays a key role in the human driver perception, since it provides most of information for further prediction and planning tasks in driving.

We collected a total of 4,300 video clips of traffic accidents in various scenarios in China (including urban, suburbs, villages and highways), which happened in 4 consecutive months from March 22, 2020 to July 27, 2020 [30]. To investigate the causes of all accidents, we reviewed the scenarios, including the road/traffic conditions and the vehicle-driver behaviors. The total 530 accidents involving vehicle-vehicle interactions, as shown in Figure 1, were labelled according to their main causes as: (1) dangerous driving behaviors (e.g., emergency braking, crossing multiple lanes in one movement, tailgating), (2) dangerous road sections (e.g., sharp turn, unsignalized intersection, merging ramp), and (3) visual blind zones (e.g., limited view via the rearview mirror, dynamic blind zone due to driver head rotation).

From Figure 1a, we find that dangerous driving behaviors account for more than 65% of accidents, however, visual blind zones also contribute to about 22% of accidents, half of which involve heavy trucks, as shown in the example cases of Figure 1b. It is understandable that for truck drivers, it is more difficult to achieve sufficient searching for visual information, as also pointed out by Larsen [31]. Considering the greater severity of truck-involved collisions, safe interaction with truck drivers must be guaranteed in AVs.

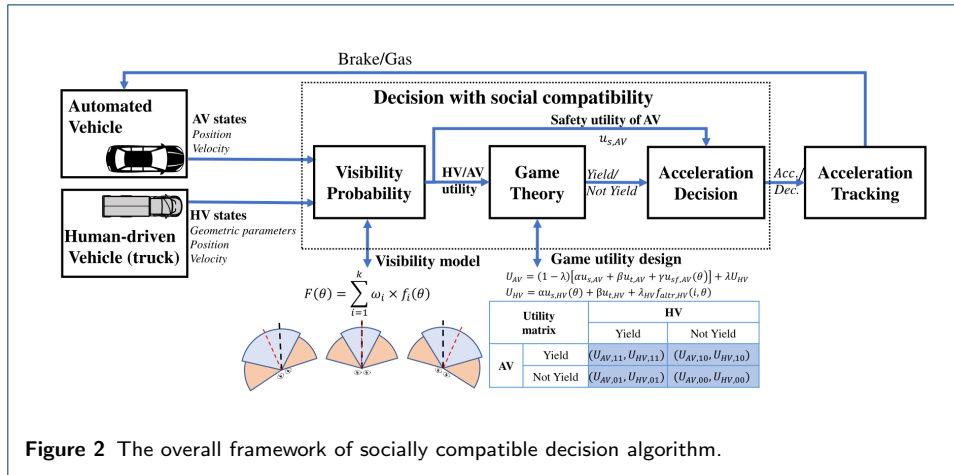
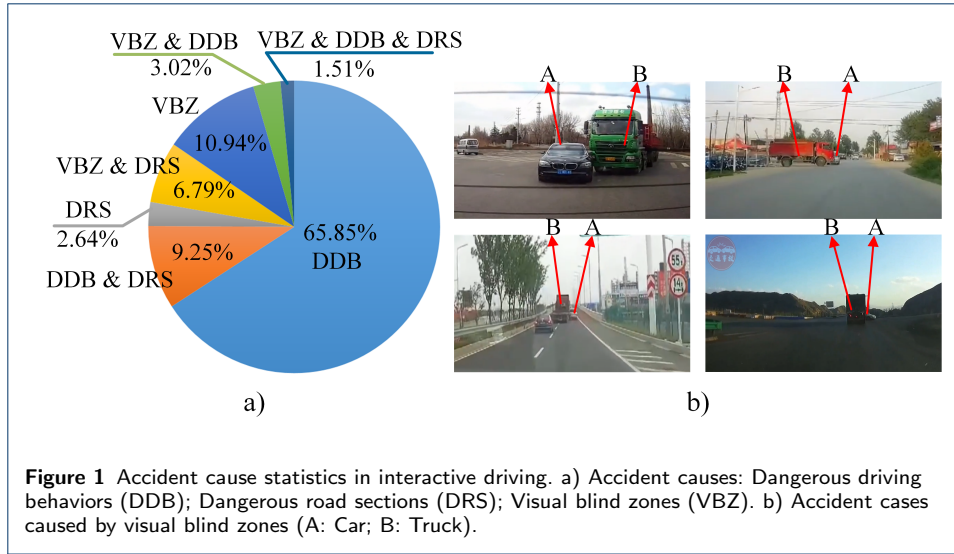
When it comes to unsignalized intersections, these visual limitations of human drivers make the interactive driving even more accident-prone. On one hand, in such dynamic driving situations it is challenging for drivers to get accurate perception of the right of way, either of the ego or interacting vehicles. On the other hand, the priority rules to guide vehicle interaction are not clearly predetermined by traffic regulations. In such situations, the aggravated complexities of intersection interactions are safety challenges that AVs have to overcome, especially in those countries and regions that do not strictly enforce the stop or yield sign regulation.

Based on these findings, we believe that the influences of HV driver visual field characteristics should be considered to realize AV's social compatibility in interactive driving.

2.2 Framework

To achieve social compatibility, including social fitness and reciprocity, the AV decision algorithm should (1) promote the HV driver's understanding of the AV intention, (2) behave with consistency and cooperate tacitly with HV, (3) and consider HV's interests while guaranteeing AV's own interests.

For the unsignalized intersection scenario, a socially compatible decision framework based on game theory is proposed, as illustrated in Figure 2.2.



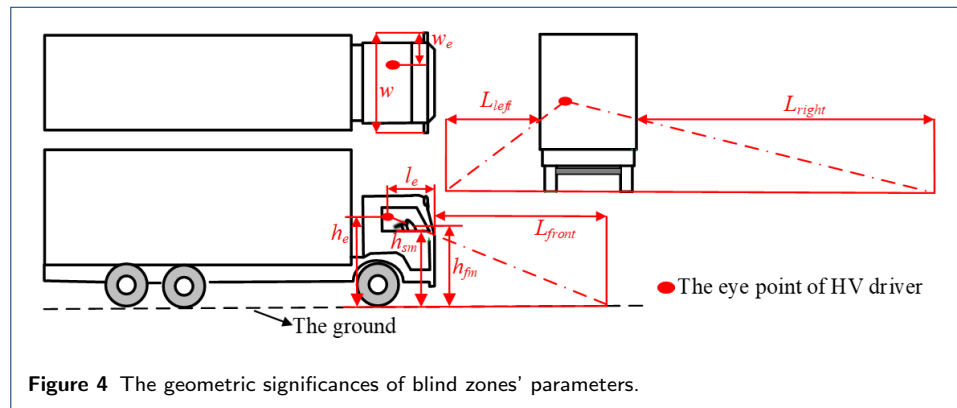
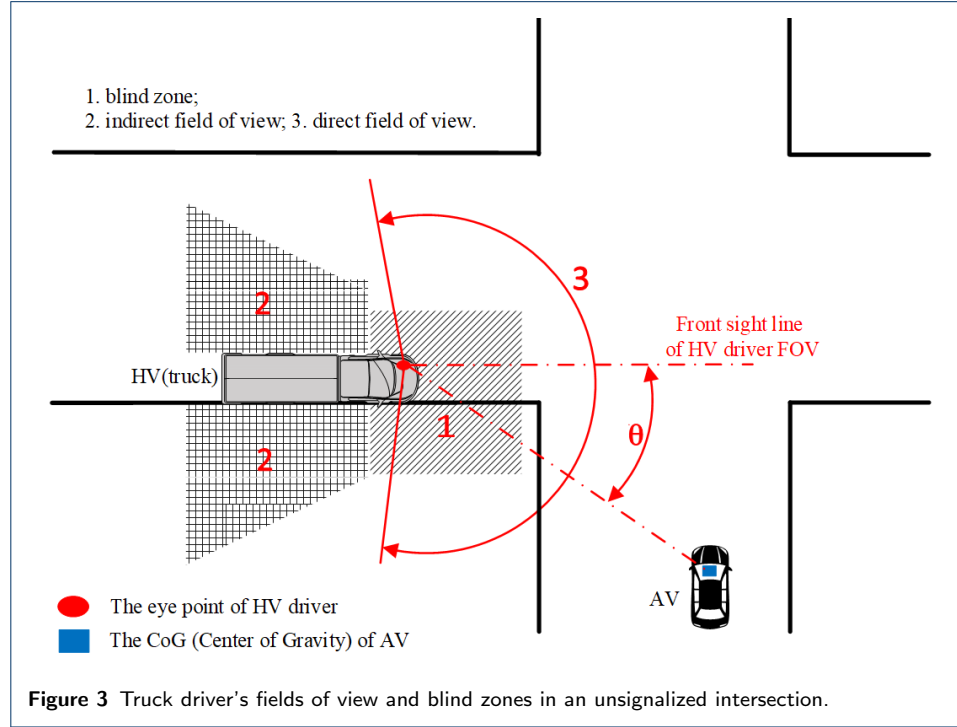
- 1 The inputs of the proposed algorithm consists of two parts, the sensing data of AV states (i.e., position and velocity) and HV states (i.e., geometric parameters, position and velocity).
- 2 Based on the sensing data, a visibility probability model is adopted to estimate the truck driver's visual characteristics, which outputs the probability of AV being observed by the HV driver.
- 3 Then, with the designed HV/AV utilitis, the decision game of AV and HV considers safety, efficiency and also social compatibility is solved, which finally outputs a decision of acceleration or deceleration.
- 4 Finally, the output decision is executed by the lower level controller.

2.3 Probabilistic model of AV visibility

The two-vehicle interaction in an unsignalized intersection is taken as an example scenario, where the HV is a heavy truck and the ego AV is a passenger vehicle, as schemed in Figure 3. The 360-degree vision of truck drivers can be divided into the blind zones, the direct and indirect fields of view. The direct field of view is the area that can be seen without the aid of any devices. The blind zone is an area around

the vehicle that cannot be directly observed when the driver is in a normal sitting position. The indirect field of view can only be seen by using auxiliary devices, e.g. rear-view mirrors. Considering the example intersection, only the blind zone and the direct field of view, i.e. areas 1 and 3, need to be modeled.

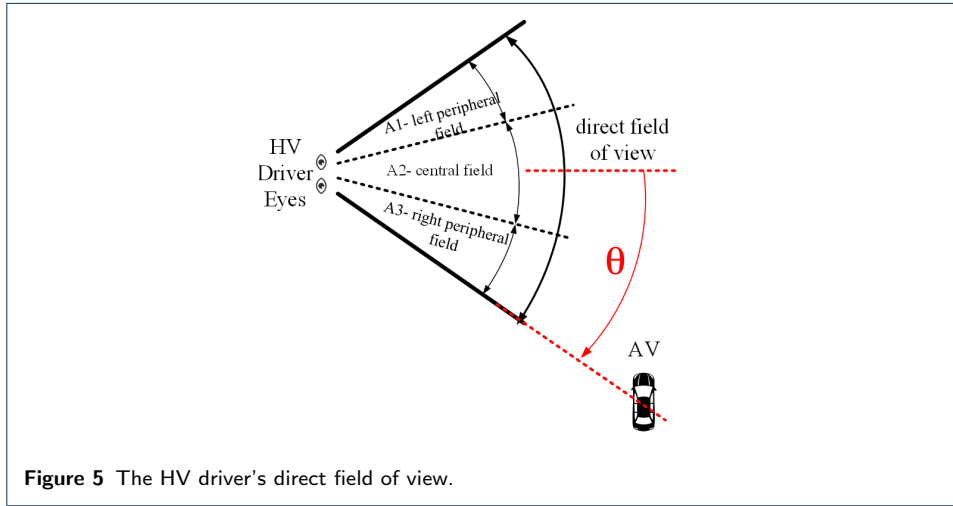
With simplification, the blind zone is defined with 3 parameters, as shown in Figure 4. L_{left} and L_{right} represent the horizontal width of the blind zone on the left/right side of the driver cabin, while L_{front} is its longitudinal length.



$$\begin{cases} L_{left} &= h_{sm} \times w_e / (h_e - h_{sm}) \\ L_{right} &= h_{sm} \times (w - w_e) / (h_e - h_{sm}) \\ L_{front} &= h_{fm} \times l_e / (h_e - h_{fm}) \end{cases} \quad (1)$$

where, w is the overall width of the cockpit, w_e is the distance between the eye point and the left side of the cockpit, and l_e is the distance between the eye point and the front end of the cockpit. h_{sm} indicates the vertical distance from the bottom edge of the side window to the ground. h_{fm} represents the height of the bottom edge of the windshield/center stack, which blocks the driver's front line of sight. h_e means the vertical distance from the driver's eye point to the ground.

For the intersection scenario, we assume that both AV and HV travel straight, i.e., HV goes from left to right, and AV goes from bottom to top, and only the AV visibility for areas 1 and 3 in Figure 3 are calculated. When AV is in the blind zone of HV driver, the probability of AV being observed by HV driver is assumed 0. For the front direct field of view (area 3), we further divide it into (A1) the left peripheral, (A2) the central and (A3) the right peripheral sub-fields, as shown in Figure 5.

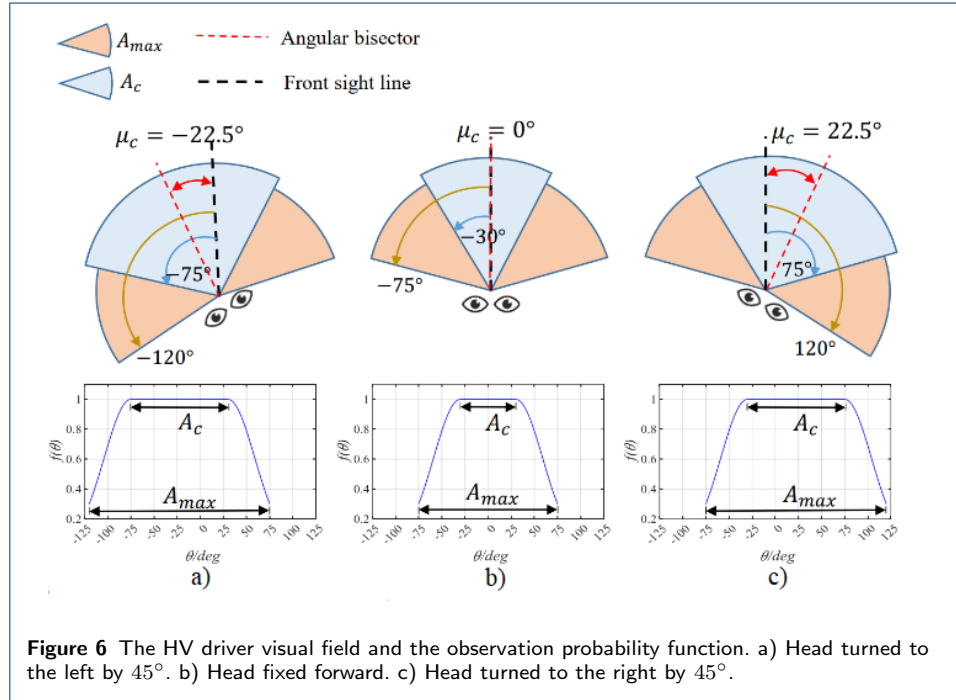


Assuming that there are normally three natural combinations of head-eye rotation of drivers. (1) If to pay attention to the left, head rotates naturally to the left and eyes rotate freely. (2) If to pay attention to the center, head keeps straight forward and eyes rotate freely. (3) If to pay attention to the right, head rotates naturally to the right and eyes rotate freely. Then the AV's visibility probability $F(\theta)$ is estimated as follows.

$$F(\theta) = \sum_{i=1}^3 \omega_i f_i(\theta), \quad (2)$$

where θ is the viewing angle of AV from the perspective of HV driver. The first part, ω_i , is the probability of HV driver paying attention to the left ($i = 1$), center ($i = 2$) or right ($i = 3$) directions. The probability ω_i is related to whether there is an object worthy of attention in the specific direction. For the intersection scenario shown in Figure 3, 162 cases from the "DADA-2000" dataset [32] are extracted, and then the probabilities ω_1 , ω_2 , ω_3 are determined according to the statistical results, which are 0, 0.17 and 0.83, respectively. When HV driver pays attention to the i th

direction, $f_i(\theta)$ is the observation probability function, representing the probability of AV being observed by the driver, as shown in Figure 6.



Human visual observation is affected by the dynamic characteristics of eyeballs. For instance, the macula is located in the optical central area of eye, and its central depression part is the most sensitive area of vision to capture dynamic objects. Therefore, the observation probability function $f_i(\theta)$ in Eq. 2 is defined as follows.

$$f_i(\theta) = \begin{cases} \xi, & \theta \in A_c \\ \xi P(\theta), & \theta \in A_{max} - A_c, \end{cases} \quad (3)$$

where A_{max} is the front direct field's angular range scanned by driver head rotation, and A_c is the central sub-field's angular range scanned by head rotation. ξ is a compensation coefficient to consider the environmental factors of the visual capturing ability, e.g. velocity, color and lighting. When AV is in the peripheral sub-fields of view, the AV observation probability of $P(\theta)$ is estimated with the following exponential function.

$$P(\theta) = p_{min}^{[(2|\theta - \mu_c| - A_c)/(A_{max} - A_c)]^2}, \quad (4)$$

where μ_c is the angle between the angular bisector and the front sight line. p_{min} is a minimum visibility probability of AV when it is at the boundary of driver's peripheral sub-field. If the driver's head is naturally turned to the left or right, an angle of 45 degrees is supposed, then $p_{min} = 0.3$, and the HV driver visual field and the observation probability function $f_i(\theta)$ of AV are schemed in Figure 6.

2.4 Game design considering social compatibility

The intersection decision game is formulated as a static game, which contains the following elements: the players (AV, HV), the strategy set (Yield, Not Yield) and the utility set (U_{AV}, U_{HV}) . The utility matrix is shown in Table 1, where $(U_{AV,mn}, U_{HV,mn})$ is the utility set if AV takes strategy m and HV takes strategy n .

Table 1 The utility matrix of the proposed decision-making algorithm

	Utility	HV	
		Yield(1)	Not Yield(0)
AV	Yield(1)	$(U_{AV,11}, U_{HV,11})$	$(U_{AV,11}, U_{HV,11})$
	Not Yield(0)	$(U_{AV,01}, U_{HV,01})$	$(U_{AV,00}, U_{HV,00})$

AV utility

To achieve safety, traffic efficiency, and also social compatibility, the AV utility U_{AV} is constructed as follows

$$U_{AV} = (1 - \lambda)[\alpha u_{s,AV} + \beta u_{t,AV} + \gamma u_{sf,AV}(\theta)] + \lambda U_{HV}, \quad (5)$$

where $u_{s,AV}$ and $u_{t,AV}$ are the safety and traffic efficiency utilities of AV, respectively. Social compatibility is represented by both the social fitness utility function $u_{sf,AV}$ and the reciprocal utility, i.e. the HV utility U_{HV} . $\alpha, \beta, \gamma, \lambda$ are the corresponding weights to trade-off among utilities. The AV position variable θ is used to consider the AV visibility, as shown in Figure 5.

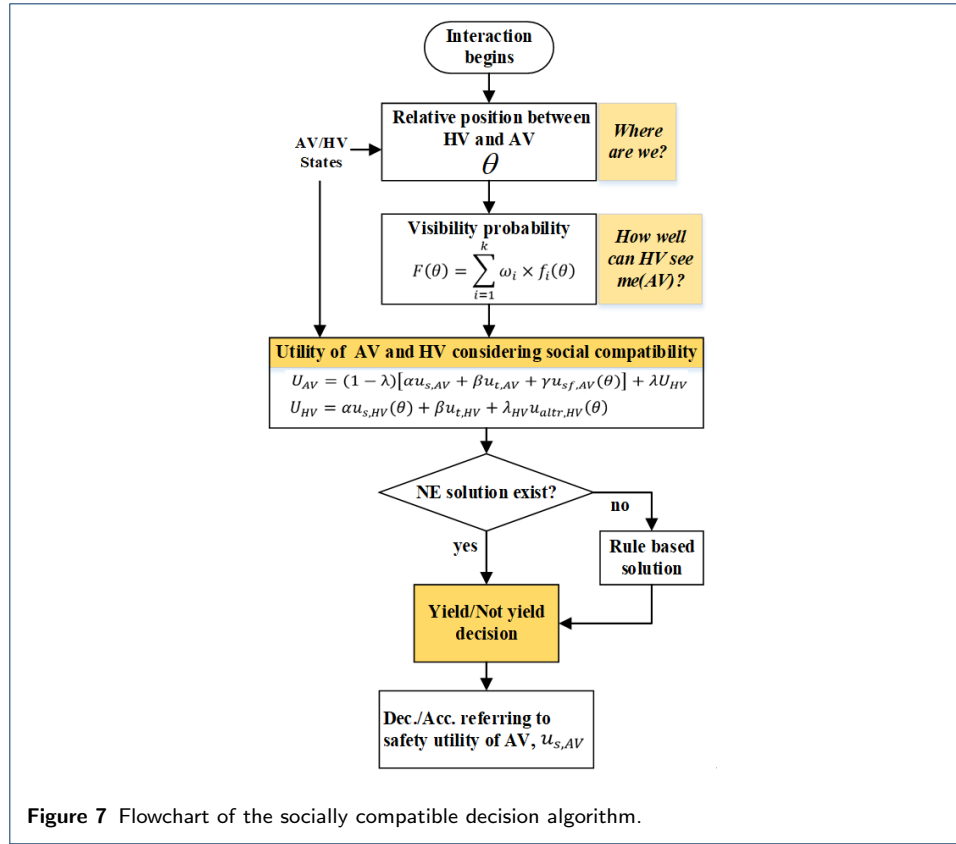
HV utility

Considering safety, traffic efficiency and reciprocal behavior, the HV utility U_{HV} is designed as

$$U_{HV} = \alpha u_{s,HV}(\theta) + \beta u_{t,HV} + \lambda_{HV} u_{altr,HV}(\theta). \quad (6)$$

where $u_{sf,HV}$ and $u_{t,HV}$ are the safety and traffic efficiency utilities of HV, respectively. $u_{altr,HV}$ is the reciprocal utility of its altruistic behavior, which is weighted by λ_{HV} . When HV driver yields to AV, the value of λ_{HV} is equal to λ in Eq. 5. If the driver does not give way to AV, λ_{HV} is 0. The utility functions of AV and HV are further explained in Appendix A. The calibration of parameters, e.g. weighting factors and thresholds, is achieved via randomly-sampled simulations.

To summarize, the flowchart of our socially compatible decision algorithm is presented in Figure 7. Firstly, the relative position between vehicles is obtained, and is used to calculate the visibility probability of AV. Then, the game utilities are calculated and used to find the Nash Equilibrium (NE) solution. Finally, the specific acceleration/deceleration of AV is decided by combining the yield decision and the safety utility of AV.



3 Human-in-the-loop experiments

3.1 Benchmark algorithms

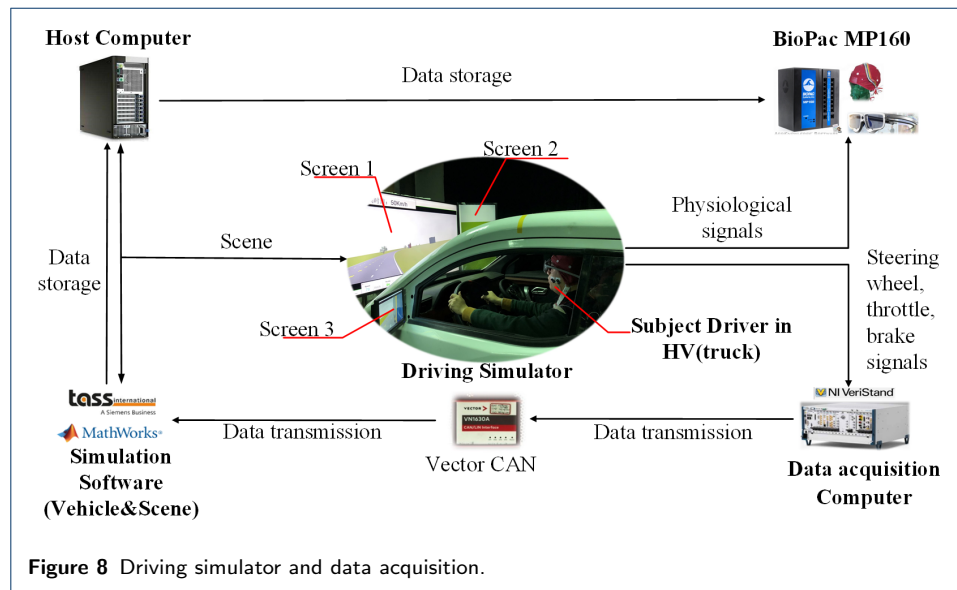
Two benchmark decision algorithms are selected to compare with the proposed socially compatible (SC) algorithm. One is the game-based algorithm that only considers safety and traffic efficiency (noSC algorithm), i.e. $\gamma = \lambda = \lambda_{HV} = 0$. The other benchmark algorithm is Responsibility Sensitive Strategy (RSS) by Intel Mobileye, which defines a set of safety rules to guarantee "it won't lead to accidents of the autonomous vehicle's blame" [33]. RSS is also one of the most popular algorithms that are currently adopted in the academia and industry. The adopted RSS model parameters are listed in Table 2. The parameter $a_{brake,min}^{HV}$ is determined according to the results of natural driving study in China [34].

Table 2 The parameters in RSS decision algorithm

Parameter	Definition	Value
ρ_{AV}	Response time for AV	0.5s
ρ_{HV}	Response time for HV	2s
$a_{accel,max}^{AV}$	Maximum acceleration for AV	3.5m/s ²
$a_{accel,max}^{HV}$	Maximum acceleration for HV	3m/s ²
$a_{brake,min}^{AV}$	Minimum deceleration for AV	-3m/s ²
$a_{brake,min}^{HV}$	Minimum deceleration for HV	-4.43m/s ²
$a_{brake,max}^{AV}$	Maximum deceleration for AV	-5m/s ²
$a_{brake,max}^{HV}$	Maximum deceleration for HV	-8m/s ²

3.2 Apparatus

As shown in Figure 8, a driving simulator with six degrees of freedom is used as the human-driven truck (HV). The simulator cabin is modified to better reproduce the driver visual limitations in the real truck cabin. The real-time simulation is based on MATLAB and TASS PreScan. The human drivers' inputs in simulator cabin, i.e. steering, throttle and brake, are collected for the vehicle dynamic model in PreScan, while the AV algorithm in MATLAB outputs the interaction decisions. The data of subject Electroencephalogram (EEG) at Fz and Cz positions are recorded and analyzed with BioPac MP160.

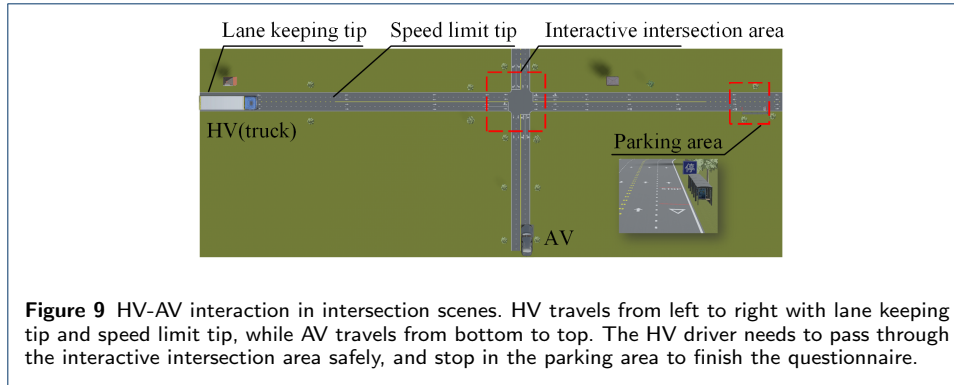


3.3 Participants and experiment design

We recruited 24 subjects of age between 21 and 28, including 22 males and 2 females. They were asked to drive as in daily driving and to interact with AVs deployed with 3 different decision-making algorithms, namely, 1) noSC algorithm, 2) RSS algorithm, 3) SC algorithm. Three different speed limits were specified, i.e. 20km/h (Lowspd), 45km/h (Midspd), 70km/h (Highspd), respectively. For each algorithm, subjects were asked to drive under specific speed limits in the rightmost lane and to complete 9 HV-AV interactions. When the HV truck was 120 meters away from the conflict area, the AV started with the *same* speed of the truck, to simulate the intense levels of interaction conflict. Once the truck was 100 meters away from the conflict area, the decision algorithm was triggered ON. After each intersection, the HV stopped at the parking area and the subject filled the questionnaire to evaluate the last AV-HV interaction, as detailed in Appendix I.B. Figure 9 presents an example of intersection scenario in the experiments.

Considering that the physiological data may have a large fluctuation during the interaction and need time to return to a stable state [35], the subjects used 3 ~ 5 minutes for free driving before the next interaction.

An experiment for each subject HV driver took about 90 minutes. The experimental procedure is as follows.



- 1 Subject fills in the driver self-ability [36] and driving style assessment questionnaires [37, 38].
- 2 Subject wears the physiological acquisition devices and confirms the signal recordings.
- 3 Subject gets familiar with the simulator driving without interaction with AVs.
- 4 The formal experiment begins, subject conducts the *Lowspd* experiment. After each interaction, a subjective questionnaire of driving tasks is filled.
- 5 Subject completes *Midspd* and *Highspd* experiments as step 4.
- 6 Subject finishes the experiments and takes off the physiological acquisition devices.

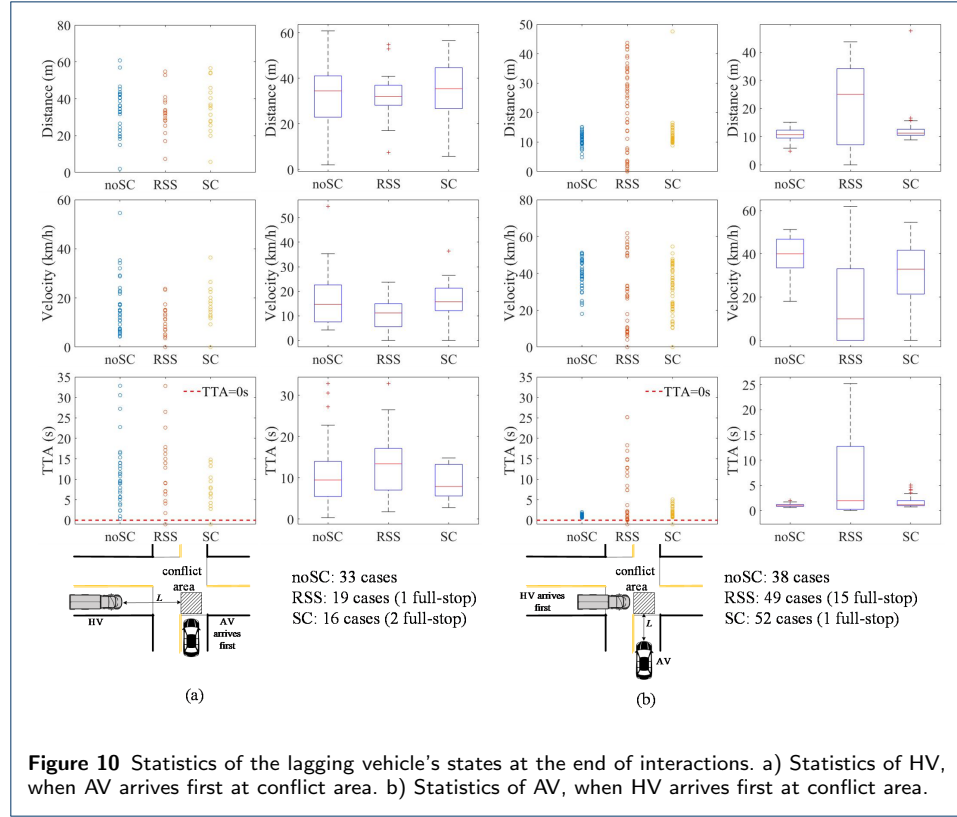
4 Results and discussion

Totally 216 interaction cases are obtained, including 207 effective interactions without collisions and 9 failed interactions due to HV's severe overspeed behaviors (more than 15km/h over limit). For detailed analysis, we further divide the interactive cases into 4 speed intervals according to the initial speed triggered by the algorithm, i.e. *Low* ($10 - 30\text{km/h}$), *LowMid* ($30 - 40\text{km/h}$), *Mid* ($40 - 50\text{km/h}$) and *High* ($50 - 70\text{km/h}$). Note that the extreme interaction cases with *High* initial speeds are rare but still possible in real traffic scenarios, which brings severe time pressure to both human drivers and AV algorithms.

4.1 Statistical analysis of safety and efficiency

To focus on the intersection interactions, we assume that the inter-vehicle interaction ends when one of the vehicles reaches the conflict area, while the following-up behaviors are not further considered. Therefore, the Time to Arrive (TTA) is selected as the safety evaluation index. When the leading vehicle, either AV or HV, arrives at the conflict area at time t , and the lagging vehicle with a speed v is still L distance away from the conflict area, then $\text{TTA} = L/v$. If TTA is large, it means when the leading vehicle arrives at the intersection, the lagging vehicle is still far away, so safety can be guaranteed. However, if TTA is too large, the traffic efficiency is compromised since the lagging vehicle is too conservative to make use of the cleared intersection space. Note that if the lagging vehicle fully stops to show its courtesy, a special value $\text{TTA} = -1$ is given rather than infinity, and such case is tagged as 'full-stop'. On the other hand, a small TTA means that both vehicles cross the intersection at a very close moment. If TTA is less than a specified

threshold, for safety the AV decision algorithm will be overridden by automated emergency braking (AEB) [34]. Such case is defined as a *danger* case. Considering the extreme inter-vehicle interactions with high initial speeds, the goal is to minimize the number of danger cases, if not possible to completely avoid all danger cases.



Statistics of all interaction cases are summarized in Table 3. In the low speed scenarios, there are 6 danger cases with the noSC algorithm, and no danger case with RSS or SC algorithms. In medium and high speed scenarios, the numbers of danger cases with noSC, RSS and SC algorithms are 9, 11 and 6, respectively. The RSS algorithm seems conservative by showing the most courtesy behaviors, i.e. 16 full-stop cases. However, it still causes 11 danger cases. Therefore, although RSS is not responsible for any collisions, i.e. the interacting HVs bear the responsibility, it is not the safest algorithm for the studied intersection driving scenarios. By contrast, the SC algorithm can achieve the best safety performances in AV-HV interactions, with no danger case with initial speeds below 40km/h and 6 danger cases with initial speeds between 40 and 70km/h .

In 207 effective cases, the distance L , speed v and TTA of the lagging vehicle at the end of the interactions are summarized in Figure 10. The cases when the AV or the HV arrives at the conflict area first are given in Figure 10a and Figure 10b, respectively. As shown in Figure 10a, when interacting with the RSS-based AV, the HV has the lowest ending velocity and its average TTA is larger than 10s, meaning that HV is the most conservative with lowest traffic efficiency. When interacting with the noSC-based AV, the efficiency of HV is improved, but there

Table 3 Statistics of interaction cases (Danger: AEB activated, Full Stop: Yield)

	# of cases	Low	Low-Mid	Mid	High
noSC	Total	22	15	26	8
	Danger		6		9
	Full Stop		0		
RSS	Total	20	12	27	9
	Danger		0		11
	Full Stop		16		
SC	Total	17	15	25	11
	Danger		0		6
	Full Stop		3		

are some extremely conservative or radical cases, that is, its TTA is either too large or too small. When interacting with the SC-based AV, the average TTA of HV is the lowest, indicating the best traffic efficiency. Also, the SC-based AV facilitates the interacting HV to have its lower bound of TTA larger than that with the other two algorithms, showing its best safety performance of HV.

For the cases when HV arrives at the conflict area first, shown in Figure 10b, it can be found that RSS-based AV is the most conservative, having the lowest traffic efficiency among all algorithms. The widely-distributed TTA values indicate that RSS performs not stably or consistently in interacting with human drivers. Part of the reason is that RSS decides with a strict sense of right of the way (RoW), which may not always be precisely followed by human drivers. In highly-dynamic interactions, human drivers are not sensitive enough of their RoW. Such problem is getting worse if a human driver has visual limitations in sensing other interacting vehicles approaching the intersection, as the truck drivers in our experiments. This unclear sense of RoW may lead to the ineffective communication between HV and AV, causing the RSS-based AV to switch frequently between 'To Go' and 'Not to Go' decisions. Based on the results of TTA and ending velocity distribution of AVs in Figure 10b, the SC algorithm can provide the AV with the best tradeoff between safety and efficiency.

4.2 Interaction case studies

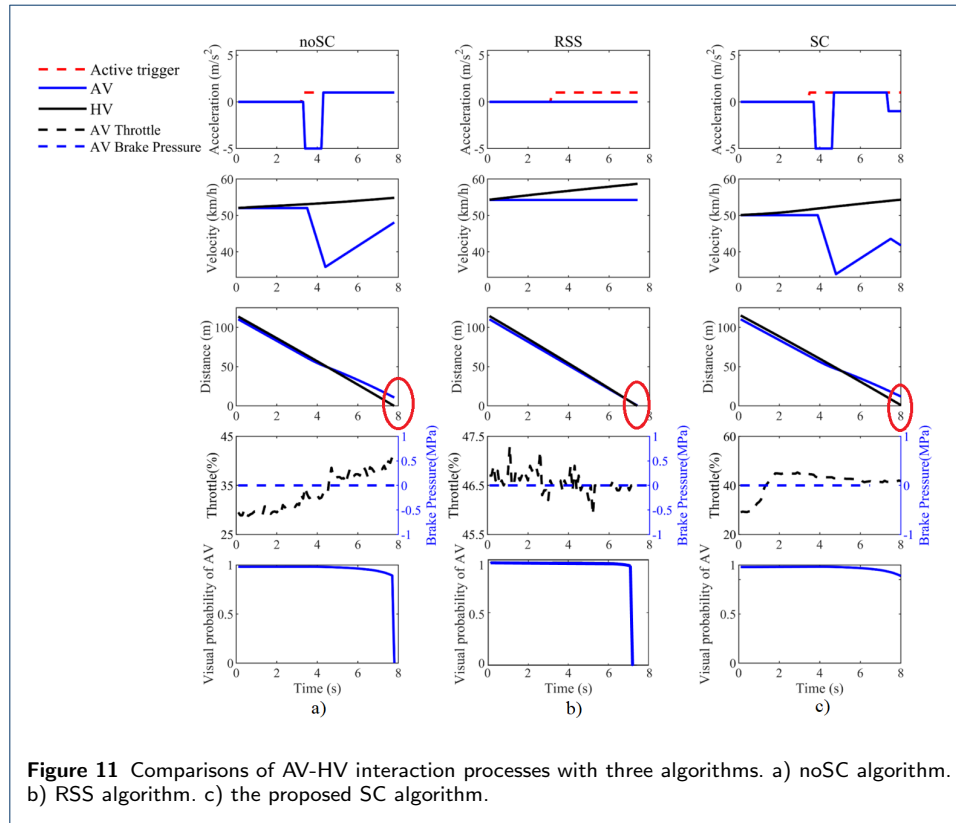
To explain the benefits of social compatibility, we select three interaction cases with similar initial speeds, i.e. 52.0km/h (noSC), 54.3km/h (RSS) and 50.1km/h (SC). For the HV in all three cases, the driver's throttle input fluctuates between $30\% \sim 45\%$, the vehicle acceleration fluctuates between $0.1 \sim 0.15\text{m/s}^2$, and the speed increment is between $3 \sim 4\text{km/h}$.

Figure 11 presents the two vehicles' states, the AV inputs, as well as the AV visibility probability estimated using 2. Since the noSC algorithm cannot consider the influence of HV visual limitations, the AV enters the blind zone of HV driver at the end of the interaction, with its visibility probability dropping to 0. The resulting TTA is 0.79s , which is less than the specified threshold of 0.83 and triggers the AEB braking.

As for the RSS case, the AV maintains the no-braking strategy according to the principle of right of way priority, but the HV does not slow down and yield according to the rules of the RSS, which finally leads to an almost inevitable collision (TTA= 0.02s). When the RSS-based AV is close to the intersection, it enters the blind zone of the HV driver, and its visibility probability drops to 0. Therefore, if

HV follows the rule of right of way priority, the RSS algorithm can achieve a safe interaction, otherwise a collision accident may happen. In the latter case, the RSS algorithm still do not lead to any accidents of AV's blame, but the accident still happens, showing that RSS is pursuing an egoism strategy and needs improvements for interaction-intensive driving.

By contrast, since the SC algorithm can directly consider the HV driver's visual limitations, the SC-based AV decelerates at $t = 7.5s$ to keep away from the blind zone of HV driver. At the end of the interaction, its visual probability is 0.85, which is still a high probability of AV being observed by the HV driver. At the end of the interaction, TTA is 0.95s, meaning a safe and efficient interaction with HV.

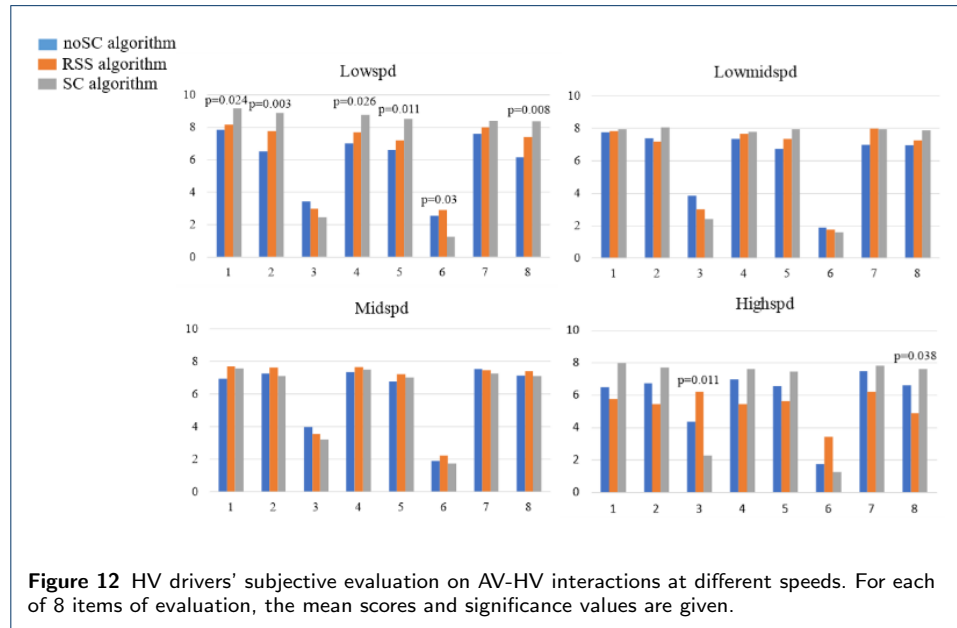


Together with the statistical results in Section 4.1, it is validated that by considering the social compatibility from the perspective of HV driver's visual limitation, the proposed decision algorithm can achieve both safety and efficiency.

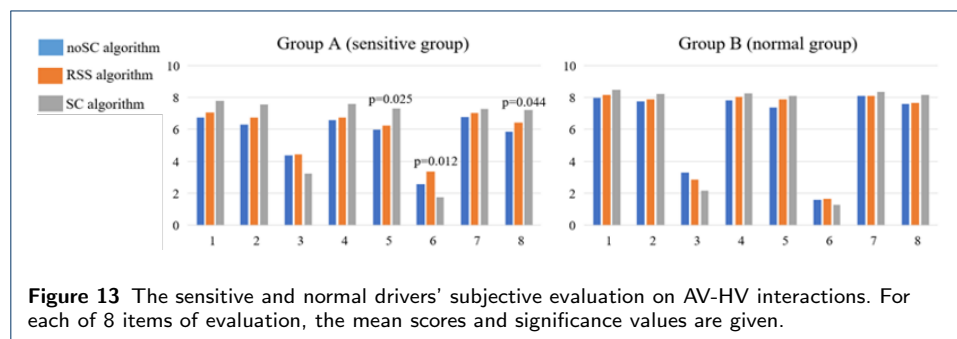
4.3 Subjective evaluation

The HV drivers' evaluations on AV are obtained via questionnaires in Table B.1. Figure 12 presents the mean and significance values of subjective evaluation on interactions, with all significance levels ($p < 0.05$) indicated for corresponding question items. It shows that, in all speed scenarios, the SC algorithm has better evaluation scores than the noSC algorithm in all items but item 2 '*comfort*' and item 7 '*calmness*'. In *High* speed scenarios, the SC algorithm performs better in all items than the noSC and RSS algorithms, with two items with significant improvements. By contrast, in *Low* speed scenarios, the SC algorithm shows the most significant

improvements in 6 evaluation items. One possible reason is that if given a specified decision step size, there are more frequent interactions in a lower-speed interaction case. This makes the subjects easier to tell the differences among the three decision algorithms, so the advantages of the SC algorithm are more obvious.



When examining those subjects who gave significantly unsatisfactory evaluations than average, we find that they have one or more of the following characteristics in driver self-ability assessment, i.e. poor driving ability, aggressive driving style, being prone to anger, or careless driving. A total of 12 subjects with the above characteristics are named Group A (sensitive), and the rest are classified into Group B (normal). The mean values and significance results of Groups A and B are shown in Figure 13. With the SC algorithm, the evaluation items 5 '*relaxed*', 6 '*confused*' and 8 '*happy*' are significantly improved for the sensitive subjects. By contrast, such improvements are not statistically significant for the normal subjects. It may be because Group A subjects are more sensitive to the process of dynamic interaction, and their mood fluctuations are more susceptible to the driving behaviors of interacting vehicle.



4.4 HV driver EEG

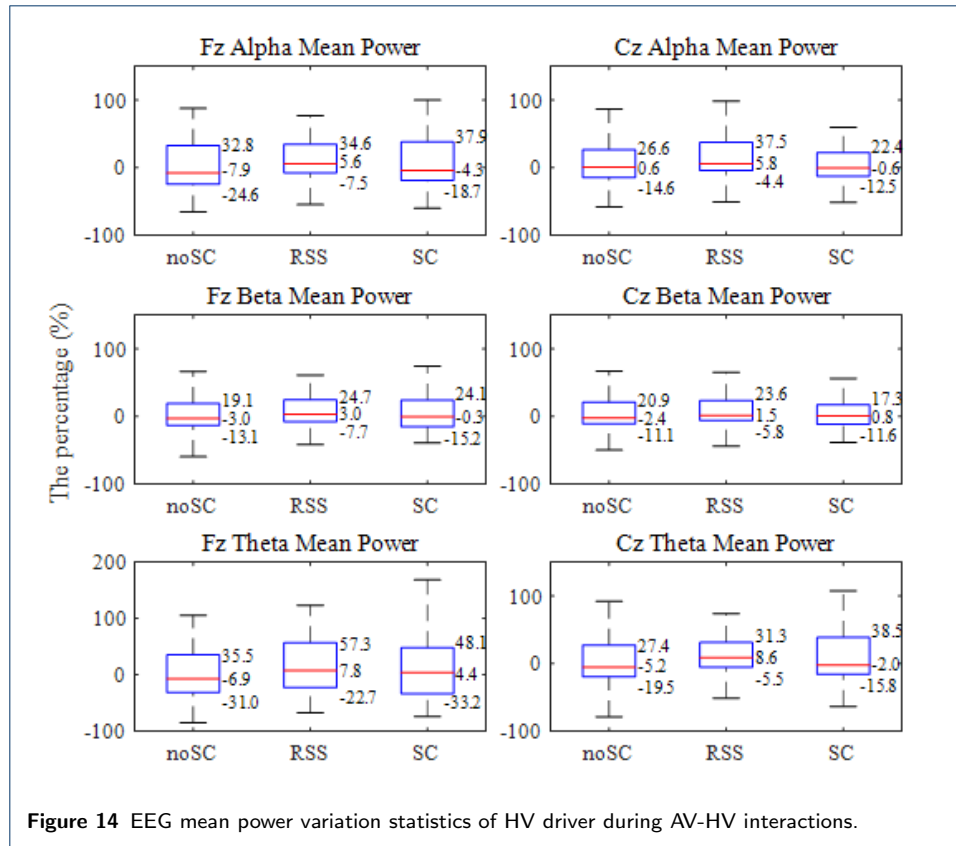
The EEG data at Fz and Cz are tagged with three stages. The *Baseline* data correspond to the stage before the AV decision algorithm is activated ON, which are considered as the EEG data before the interaction. The *Interaction* data correspond to the stage of interaction, i.e. when the HV drives from 120m away from the conflict area to the end of interaction. The *After* data correspond to the stage of 6s after the interaction. For the EEG signal features, the mean power values of Alpha (8 ~ 13Hz), Beta (13 ~ 30Hz) and Theta (4 ~ 8Hz) waves are extracted to judge the subjects' emotion fluctuation. For each of the total 24 subjects, the EEG results during interactions for one speed limit are taken as a data group. Finally, 61 effective data groups are obtained by eliminating the failed group, including those with over speed driving or lost EEG signals.

Cao [39] pointed out that the power of Alpha and Theta waves increases when user feels more pleasure, and the power of Beta wave rises with the enhancing of positive emotions. Here, for the 61 effective data groups, with the power analysis of Alpha, Theta, and Beta waves, it is found that in 44 data groups, i.e. 72%, the EEG evidences can confirm the driver emotion changes represented by the corresponding subjective evaluation (items 2, 4, 5 and 8). In the rest of 17 data groups, the EEG results are not consistent with the subjective evaluation.

For the 61 effective groups of EEG data, the variation percentage of EEG mean power in each interaction is defined as $GR = (P_{base} - P_{int}) / P_{base} * 100\%$, where P_{base} represents the mean power in the *Baseline* stage, P_{int} represents the mean power in the *Interaction* stage. The statistical results are shown in the Figure 14. It is found that when subjects interact with the AVs with the RSS and SC algorithms, the mean power values of all EEG features are higher than those with the noSC algorithm. This confirms the subjective evaluation results that when interacting with the noSC algorithm, the satisfaction level of the subjects is lowest. By contrast, by considering social compatibility, the SC algorithm can provide an equivalent level of satisfaction as the conservative RSS algorithm.

The findings of human-in-the-loop experiments of AV-HV interactions can be summarized as follow.

- 1 Compared to the other benchmarks, the proposed SC algorithm can better balance safety and traffic efficiency, and achieve smoother interactions between AV and HV.
- 2 From the microscopic case studies, the consideration of human visual limitations and social compatibility can help avoid less effective interactions due to blind zones, which can better improve safety.
- 3 When the AV with our SC algorithm interacts with human drivers, in addition to objective performances of safety and efficiency, it improves its own predictability and makes the HV drivers feel safer and clearer about the inter-vehicle interactions. This is a significant improvement over the commonly-used algorithms in current AVs. This further confirms that to be a real safe and trust-worthy traffic participant, AV should not only make decisions primly according to safety rules and the right of way, but also behave empathetically by considering other human drivers' limits of driving capabilities.



5 Conclusion

The aim of this study is to propose an unsignalized intersection decision algorithm that can achieve safety, efficiency and social compatibility during dynamic interactions with human-driven vehicles.

- 1 A probabilistic model of the interacting driver's visual limitations is constructed, which can estimate the probability of AV being observed by the human driver during the interaction process.
- 2 Based on this visibility model, social compatibility is further realized using a game-theoretic framework.
- 3 Human-in-the-loop experiments are carried out for the validation of the proposed algorithm. Results show that in addition to the well-balanced safety and time efficiency, the proposed AV decision algorithm can significantly improve social compatibility and make AV decision more in line with the expectation of human drivers.

This study is one step further towards more advanced and human-like decision algorithms for automated vehicles. However, here we focus on realizing social compatibility from the perspective of other drivers' visual perception, while in future work the AV visibility model can be improved by considering the interaction uncertainties. Additionally, the main idea of incorporating social compatibility in AV decisions may be further applied in other interacting driving scenarios.

Appendix I

A. Detailed utility functions of AV and HV

AV utility

For a given interaction process, Δt is defined as the time difference between the AV and HV's arriving time at the conflict area. By normalizing the time difference Δt , we can describe the safety utility u_s of a two-vehicle interaction process as follows, which is a value between -1 and 1. The safety utility of AV is $u_{s,AV} = u_s$, while the safety utility of HV depends on how well the AV can be observed by the HV driver.

$$f_i(\theta) = \begin{cases} \Delta t / \Delta t_{rsk} - 1, & \Delta t \in [0, \Delta t_{rsk}] \\ (\Delta t - \Delta t_{rsk}) / (\Delta t_{saf} - \Delta t_{rsk}), & \Delta t \in (\Delta t_{rsk}, \Delta t_{saf}) \\ 1, & \Delta t \in [\Delta t_{saf}, +\infty) \end{cases} \quad (7)$$

where the parameters Δt_{rsk} and Δt_{saf} are the risky and safe thresholds of time difference Δt , respectively. As shown in Figure 15, the overlapped path of interactive vehicles is defined as the conflict area. At time t_0 , if AV arrives at the conflict area first, given HV's location P_{HV0} , velocity v_{HV} , the distance to conflict area L_{HV} , the thresholds $\Delta t_{rsk}, \Delta t_{saf}$ are determined as follow. If when HV arrives at conflict area (location P_{HV1}), AV has just left conflict area meanwhile (location P_{AV1}), this time difference is defined as Δt_{rsk} . On the other hand, if AV has left the intersection (location P_{AV2}), this time difference is defined as Δt_{saf} , as shown in Eq. 10. Similarly, if HV will arrive at the conflict area at time t_0 , we can also calculate the corresponding safety utility.

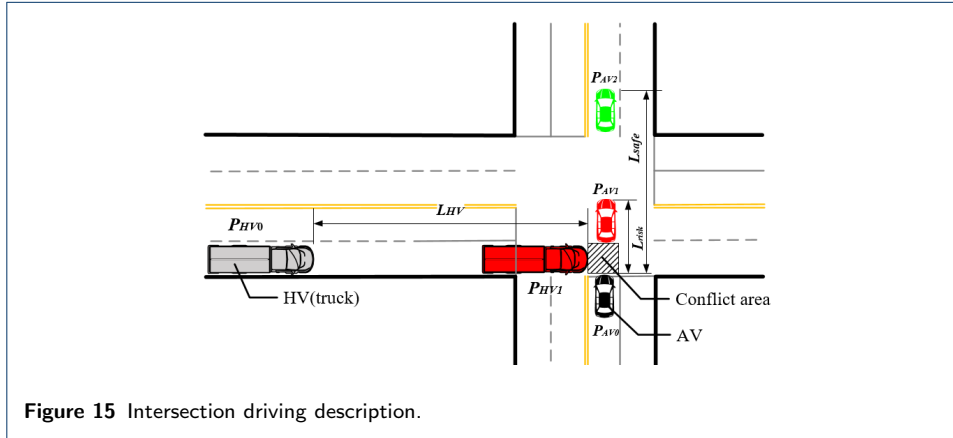


Figure 15 Intersection driving description.

$$\begin{cases} \Delta t &= L_{HV} / v_{HV} \\ \Delta t_{rsk} &= L_{risk} / v_{HV} \\ \Delta t_{saf} &= L_{safe} / v_{HV} \end{cases} \quad (8)$$

Assuming the AV distance from the conflict area at time t is L_{AV} , and the velocity is v_{AV} , then $t_{AV} = L_{AV} / v_{AV}$. If setting the maximum allowable velocity is v_{max} , an efficiency time is defined as $t_{eff,AV} = L_{AV} / v_{max}$. Then the traffic efficiency utility of AV, $u_{t,AV}$ is

$$u_{t,AV} = \begin{cases} 1 - (t_{AV} - t_{eff,AV})/t_{eff,AV}, & t_{AV} \leq t_{eff,AV} \\ 1, & t_{AV} > t_{eff,AV} \end{cases} \quad (9)$$

The social fitness utility of AV $u_{sf,AV}$ represents how much the AV decision fits to the HV decision, which is modelled in Eq. 10 with the AV visibility probability $F(\theta)$ and the tacitness degree $f_{tacit}(i, j)$. If $F(\theta)$ is small, the HV driver can hardly notice AV, so there is no cooperative driving behavior between them. The degree of tacit cooperation is explained in Table 5, in which (i, j) stand for AV and HV, respectively. When HV adopts the Yield strategy, if AV yields as well, the tacitness degree is $f_{tacit} = 0$, if AV does not yield, we set $f_{tacit} = 1$.

$$u_{sf,AV} = F(\theta)f_{tacit}. \quad (10)$$

Table 4 The tacitness degree f_{tacit} of AV under different conditions

	f_{tacit}	HV	
		Yield	Not Yield
AV	Yield	0	1
	Not Yield	1	0

HV utility

The safety utility of HV, $u_{s,HV}$ is designed as

$$u_{s,HV} = \begin{cases} (u_s)^{F(\theta)}, & u_s \geq 0 \\ (-u_s)^{F(\theta)}, & u_s < 0 \end{cases} \quad (11)$$

where the AV visibility probability $F(\theta)$ is introduced to correct the safety utility u_s . For example, when AV is in the blind zones or is almost invisible from the perspective of HV driver, it is assumed that there is no vehicle interacting with HV, and the maximum safety utility is achieved, $u_{s,HV} = 1$.

Similar to Eq. 11, the traffic efficiency utility of HV is as follows.

$$u_{t,HV} = \begin{cases} 1 - (t_{HV} - t_{eff,HV})/t_{eff,HV}, & t_{HV} \leq t_{eff,HV} \\ 1, & t_{HV} > t_{eff,HV} \end{cases} \quad (12)$$

The reciprocal utility from the HV's altruistic behavior is quantified with the traffic efficiency of AV and the AV visibility probability $F(\theta)$, i.e.

$$u_{altr,HV}(\theta) = F(\theta)u_{t,AV} \quad (13)$$

B. Questionnaire for the HV drivers' evaluation on the AV-HV interaction

Instruction for subject drivers: "Please score the items in Table 5 based on your feelings about your last interaction with the other vehicle."

Table 5 Questionnaire for evaluation on the AV-HV interaction

Evaluation item	Score
1. I feel safe in interaction	0~10
2. I feel comfortable in interaction	
3. I worry about collision with the other vehicle	
4. I feel satisfied with the interaction	
5. I feel relaxed in interaction	
6. I am confused by the behavior of the other vehicle	
7. I feel calm in interaction	
8. I feel happy in interaction	

Appendix II

Funding

This work was supported by Department of Science and Technology of Zhejiang (No. 2022C01241 and No. 2018C01058).

Availability of data and materials

A video abstract is provided, which includes a brief introduction of the proposed approach and a video of experiments. Please visit <http://b23.tv/xAOo2ib>.

Ethics approval and consent to participate

Ethics approval was obtained for this study, and all human subjects gave their informed consent.

Competing interests

The authors declare that they have no competing interests.

Authors' contributions

DL contributed in conceptualization, funding acquisition, algorithm, writing and video abstract. AL and HP contributed in algorithm, visualization, writing - review & editing, and video abstract. WC was a major contributor in methodology, algorithm, data curation and writing the original draft.

Authors' information

DL received the B.S. degree in Vehicle Engineering from the Jilin University of Technology, Changchun, China, in 2003, and the Ph.D. degree in Vehicle Engineering from the Shanghai Jiao Tong University, Shanghai, China, in 2008. He joined Zhejiang University in June 2008, first as a Post-Doc, then served as Assistant Professor, and now is Associate Professor. In 2011, he was a Visiting Scholar with the University of Missouri-Columbia, and from 2014 to 2016, he was a Visiting Scholar with the University of Michigan, Ann Arbor, Michigan. He currently directs the Research Group of Human-Mobility-Automation (<https://person.zju.edu.cn/daofei>), and his research interests include vehicle dynamics and control, automated driving and complete human-vehicle system dynamics. AL, HP and WC are graduate students in the group.

Author details

Institute of Power Machinery and Vehicular Engineering, Faculty of Engineering, Zhejiang University, No. 38 Zheda Road, Xihu District, 310027, Hangzhou, China.

References

- Kyriakidis, M., de Winter, J.C., Stanton, N., Bellet, T., van Arem, B., Brookhuis, K., Martens, M.H., Bengler, K., Andersson, J., Merat, N., *et al.*: A human factors perspective on automated driving. *Theoretical Issues in Ergonomics Science* **20**(3), 223–249 (2019)
- Manchon, J., Bueno, M., Navarro, J.: From manual to automated driving: How does trust evolve? *Theoretical Issues in Ergonomics Science* **22**(5), 528–554 (2021)
- Liu, S.: Optimization of intelligent driving decision algorithm for trust enhancement. Master Thesis, Zhejiang University (2021)
- Xu, Z., Jiang, Z., Wang, G., Wang, R., Li, T., Liu, J., Zhang, Y., Liu, P.: When the automated driving system fails: Dynamics of public responses to automated vehicles. *Transportation Research Part C: Emerging Technologies* **129**, 103271 (2021). doi:10.1016/j.trc.2021.103271
- Yu, B., Bao, S., Zhang, Y., Sullivan, J., Flannagan, M.: Measurement and prediction of driver trust in automated vehicle technologies: An application of hand position transition probability matrix. *Transportation Research Part C: Emerging Technologies* **124**, 102957 (2021). doi:10.1016/j.trc.2020.102957
- Noy, I.Y., Shinar, D., Horrey, W.J.: Automated driving: Safety blind spots. *Safety Science* **102**, 68–78 (2018). doi:10.1016/j.ssci.2017.07.018
- Li, S., Shu, K., Chen, C., Cao, D.: Planning and decision-making for connected autonomous vehicles at road intersections: A review. *Chinese Journal of Mechanical Engineering* **34**(1), 1–18 (2021)
- Di, X., Shi, R.: A survey on autonomous vehicle control in the era of mixed-autonomy: From physics-based to ai-guided driving policy learning. *Transportation Research Part C: Emerging Technologies* **125**, 103008 (2021). doi:10.1016/j.trc.2021.103008
- Schwall, M., Daniel, T., Victor, T., Favaro, F., Hohnhold, H.: Waymo public road safety performance data. *arXiv* (2020). doi:10.48550/ARXIV.2011.00038
- Schwartz, W., Alonso-Mora, J., Rus, D.: Planning and decision-making for autonomous vehicles. *Annual Review of Control, Robotics, and Autonomous Systems* **1**(1), 187–210 (2018). doi:10.1146/annurev-control-060117-105157

11. Beaucorps, P., Streubel, T., Verroust-Blondet, A., Nashashibi, F., Bradai, B., Resende, P.: Decision-making for automated vehicles at intersections adapting human-like behavior. In: 2017 IEEE Intelligent Vehicles Symposium (IV), pp. 212–217. IEEE, Los Angeles, CA, USA (2017). doi:10.1109/IVS.2017.7995722
12. Chen, J., Yuan, B., Tomizuka, M.: Deep imitation learning for autonomous driving in generic urban scenarios with enhanced safety. In: 2019 IEEE/RSJ International Conference on Intelligent Robots and Systems (IROS), pp. 2884–2890. IEEE, Macau, China (2019). doi:10.1109/IROS40897.2019.8968225
13. Sezer, V., Bandyopadhyay, T., Rus, D., Frazzoli, E., Hsu, D.: Towards autonomous navigation of unsignalized intersections under uncertainty of human driver intent. In: 2015 IEEE/RSJ International Conference on Intelligent Robots and Systems (IROS), pp. 3578–3585. IEEE, Hamburg, Germany (2015). doi:10.1109/IROS.2015.7353877
14. Menendez-Romero, C., Sezer, M., Winkler, F., Dornhege, C., Burgard, W.: Courtesy behavior for highly automated vehicles on highway interchanges. In: 2018 IEEE Intelligent Vehicles Symposium (IV), pp. 943–948. IEEE, Changshu (2018). doi:10.1109/IVS.2018.8500407
15. Wang, W.-J.: Decision and behavior planning for a self-driving vehicle at unsignalized intersections. In: 2020 International Automatic Control Conference (CACS), pp. 1–6. IEEE, Hsinchu, Taiwan (2020). doi:10.1109/CACS50047.2020.9289738
16. Lefkopoulou, V., Menner, M., Domahidi, A., Zeilinger, M.N.: Interaction-aware motion prediction for autonomous driving: A multiple model kalman filtering scheme. IEEE Robotics and Automation Letters **6**(1), 80–87 (2021). doi:10.1109/LRA.2020.3032079
17. Yoon, Y., Yi, K.: Design of longitudinal control for autonomous vehicles based on interactive intention inference of surrounding vehicle behavior using long short-term memory. In: 2021 IEEE International Intelligent Transportation Systems Conference (ITSC), pp. 196–203. IEEE, Indianapolis, IN, USA (2021). doi:10.1109/ITSC48978.2021.9564986
18. Wang, L., Wu, T., Fu, H., Xiao, L., Wang, Z., Dai, B.: Multiple contextual cues integrated trajectory prediction for autonomous driving. IEEE Robotics and Automation Letters **6**(4), 6844–6851 (2021). doi:10.1109/LRA.2021.3094564
19. Zhang, T., Song, W., Fu, M., Yang, Y., Wang, M.: Vehicle motion prediction at intersections based on the turning intention and prior trajectories model. IEEE/CAA Journal of Automatica Sinica **8**(10), 1657–1666 (2021). doi:10.1109/JAS.2021.1003952
20. Karle, P., Geisslinger, M., Betz, J., Lienkamp, M.: Scenario understanding and motion prediction for autonomous vehicles – review and comparison. IEEE Transactions on Intelligent Transportation Systems, 1–21 (2022). doi:10.1109/TITS.2022.3156011
21. Li, N., Yao, Y., Kolmanovsky, I., Atkins, E., Girard, A.R.: Game-theoretic modeling of multi-vehicle interactions at uncontrolled intersections. IEEE Transactions on Intelligent Transportation Systems (2020)
22. Jin, X., Li, K., Jia, Q.-S., Xia, H., Bai, Y., Ren, D.: A game-theoretic reinforcement learning approach for adaptive interaction at intersections. In: 2020 Chinese Automation Congress (CAC), pp. 4451–4456 (2020). IEEE
23. Cai, J., Hang, P., Lv, C.: Game theoretic modeling and decision making for connected vehicle interactions at urban intersections. In: 2021 6th IEEE International Conference on Advanced Robotics and Mechatronics (ICARM), pp. 874–880 (2021). IEEE
24. Chandra, R., Manocha, D.: Gameplan: Game-theoretic multi-agent planning with human drivers at intersections, roundabouts, and merging. IEEE Robotics and Automation Letters (2022)
25. Chen, W.: Research on autonomous driving decision algorithm considering social compatibility. Master Thesis, Zhejiang University (2021)
26. Wang, L., Sun, L., Tomizuka, M., Zhan, W.: Socially-compatible behavior design of autonomous vehicles with verification on real human data. IEEE Robotics and Automation Letters **6**(2), 3421–3428 (2021). doi:10.1109/LRA.2021.3061350
27. Li, D., Liu, G., Xiao, B.: Human-like driving decision at unsignalized intersections based on game theory. Proceedings of the Institution of Mechanical Engineers, Part D: Journal of Automobile Engineering (2022). doi:10.1177/09544070221075423
28. Li, D., Hao, P.: Two-lane two-way overtaking decision model with driving style awareness based on a game-theoretic framework. Transportmetrica A: Transport Science (2022). doi:10.1080/23249935.2022.2076755
29. Ladegård, G.: Forming strategic alliances: The role of social compatibility. Ph.D. Thesis, Norwegian School of Economics and Business Administration (1997)
30. Traffic accident video: Personal space of traffic accident video (2020). <https://www.acfun.cn/u/4075269> (accessed Feb. 08, 2021)
31. Larsen, L.: Methods of multidisciplinary in-depth analyses of road traffic accidents. Journal of Hazardous Materials **111**(1), 115–122 (2004). doi:10.1016/j.jhazmat.2004.02.019. A Selection of Papers from the JRC/ESReDA Seminar on Safety Investigation Accidents, Petten, The Netherlands, 12–13 May, 2003
32. Fang, J., Yan, D., Qiao, J., Xue, J., Wang, H., Li, S.: Dada-2000: Can driving accident be predicted by driver attention? analyzed by a benchmark. In: 2019 IEEE Intelligent Transportation Systems Conference (ITSC), Auckland, NZ, pp. 4303–4309 (2019). doi:10.1109/ITSC.2019.8917218
33. Shalev-Shwartz, S., Shammah, S., Shashua, A.: On a formal model of safe and scalable self-driving cars. arXiv (2018). doi:10.48550/ARXIV.1708.06374
34. Li, L., Zhu, X., Dong, X., Ma, Z.: A research on the collision avoidance strategy for autonomous emergency braking system. Automotive Engineering **37**(2), 168–174 (2015)
35. Lin, W.: Emotion recognition and application based on physiological signals. Ph.D. Thesis, Zhejiang University (2019)
36. Lajunen, T., Summala, H.: Driving experience, personality, and skill and safety-motive dimensions in drivers' self-assessments. Personality and Individual Differences **19**(3), 307–318 (1995)
37. Liu, J.: Analysis on lane changing trajectory under different driving style and design on assistant lane changing

- system. Master's Thesis, Changsha University of Science & Technology (2015)
38. Sun, Y.: Study on discretionary lane-changing behavior on urban streets. Master's Thesis, Dalian University of Technology (2017)
 39. Cao, K.: The research of the EEG frequency power features in three basic emotions. Master's Thesis, Tianjin Medical University (2019)